Journal of Applied Polymer Science

Synergistic effect of organoclay fillers based on fluorinated surfmers for preparation of polystyrene nanocomposites

Chahinez Benbayer,[1,2] Salima Saidi-Besbes,[1] Elisabeth Taffin de Givenchy,[2] Sonia Amigoni,[2] Frédéric Guittard,[2] Aicha Derdour[1]

[1]Université Oran 1 Ahmed Benbella, Laboratoire de Synthèse Organique Appliquée (LSOA), Département de chimie, Faculté des sciences exactes et appliquées, BP 1524 EL Mnaouer, 31000 Oran – Algérie

[2]Université de Nice Sophia-Antipolis, Laboratoire de Physique et de la Matière Condensée (LPMC) EA 3155, Equipe Chimie Organique aux Interfaces, Parc Valrose, 06108 Nice Cedex 2-France

Correspondence to: S. Saidi-Besbes (E-mail: saidi.salima@univ-oran.dz or salima_saidi@yahoo.fr)

ABSTRACT: Novel fluorinated reactive surfactants were used for the organic modification of monmorillonite clays. These organoclays were used for the preparation of polystyrene−clay nanocomposites by in-situ free radical polymerization. Reference systems based on hydrocarbon homologous surfmer and nonpolymerizable surfactants were also used to deduce the effect of the fluorine moiety and the polymerizable function on the morphology and thermal stability of the prepared nanocomposites. Different structural parameters of the surfactants were investigated and modulated for the clay modification including: the nature of surfactant (surfmer/classical surfactant, fluorinated, or hydrocarbonated), the length of the fluorinated chain as well as the length of the hydrocarbon spacers linking the ammonium head to the fluorine chain or the polymerizable acrylic function. Wide angle-X-ray scattering (WAXD), thermogravimetric analysis (TGA), and electronic microcopies (TEM and SEM) were used to establish a structure-morphology, thermal properties relationships, and to highlight the key parameters governing the exfoliation process. © 2015 Wiley Periodicals, Inc. J. Appl. Polym. Sci. **2015**, *132*, 42347.

KEYWORDS: clay; composites; polystyrene; structure−property relations

Received 4 December 2014; accepted 11 April 2015
DOI: 10.1002/app.42347

INTRODUCTION

Fluorinated compounds have attracted much attention due to their particular properties such as thermal, chemical, aging, weather resistance, low dielectric constant, refractive index, surface energy, and flammability.[1] They find a wide range of applications in advanced technologic domains such as automotive, aerospace industries, optics, microelectronics,[2–4] weather resistant paints, oil, water repellents, and antigraffiti coatings.[5–7]

The incorporation of this class of compounds into inorganic matrices constitutes an interesting approach to combine the benefit of fluorine moiety with those of inorganic derivatives. Super-water-repellent fluorinated inorganic−organic coating films on nylon 66 substrate were obtained from poly(methyl methacrylate) (PMMA), tetraethoxysilane (TEOS), and 2-perfluorooctylethyltriethoxysilane by the sol−gel method.[8] Polybenzimidazole (PBI)/silica nanocomposite membranes were prepared from an organosoluble fluorine-containing PBI copolymer for high-temperature proton exchange membrane fuel cells.[9]

Among the inorganic matrices used as filler to prepare hybrid organic/inorganic nanocomposites materials, clays were extensively studied.[10,11] Their layer structures based on an octahedral alumina sheet sandwiched between two tetrahedral silica sheets were adequate for the intercalation of host molecules particularly cationic molecules as alkylammonium and alkylphosphonium surfactants by cation exchange reactions with the interlayer inorganic and organic cations. The chemical modification of clays was usually used for the preparation of polymer-clay nanocomposites since it allows the enhancement of the compatibility between natural clay mineral and polymers.[12] Polymer−clay nanocomposites have attracted the interest of academics and industrialists due to their remarkable mechanical, thermal, oxygen, water permeability, and flame-retardant properties compared to the corresponding polymers. These improved properties are obtained even for composites with only 3−5 wt % clay loading.[13,14]

Different approaches were used to prepare polymer−clay nanocomposites. Melt intercalation and solution blending lead to intercalated nanocomposites in which the polymer chains are partially inserted between the clay mineral platelets.[11] The long range order of clay layers is maintained in this case.

The exfoliated nanostructures are more desirable than the intercalated ones due to the stronger interaction and synergistic effects between polymer matrix and silicate layers which enhance the thermal stability and mechanical properties of the prepared composite materials as compared to pure polymers.[15]

In situ polymerization is thought to be the most promising method to obtain exfoliated structure. In this method, clay is swollen by the monomer which enables the entry of monomer inside the clay galleries before polymerization. Different variants of in situ intercalative polymerization were used to prepare exfoliated PS/clay nanocomposites as free radical,[16] suspension,[17] and emulsion[18] polymerization. Clay fillers can be used in its natural state or modified with cationic surfactants to ensure better compatibility with polymer materials.

Highly exfoliated polystyrene-Na^+-montmorillonite nanocomposites have been prepared using Na^+-MMT clay platelets as stabilizer during suspension polymerization of styrene monomer.[17] Cationic radical initiator-MMT hybrid based on 2,2'-azobis[2-methyl-N-(2-hydroxyethyl)propionamide] was used by Uthirakumar *et al.* which enables efficient intra-gallery polymerization of polystyrene leading to exfoliated PS-MMT clay nanocomposites.[19]

The use of reactive surfactants was also investigated for the preparation of polymer−clay nanocomposite systems. Several studies showed the ability of polymerizable surfactants, known as surfmers, to form exfoliated morphologies in contrast of their homologous classic surfactants which provide composites with intercalated morphologies[18,20,21]. This has generally been attributed to the copolymerization between the main monomer and the surfmers inside the clay galleries that causes extensive movement of the clay layers, resulting in exfoliated nanocomposites.[22]

Fluorosurfactants for mineral clays modification by ionic exchanging process have been less reported in the literature.[23,24] The introduction of fluorinated surfactants into the clay interlayer gallery space should have a drastic effect on the nature of the cavity which changes from hydrophilic to hydrophobic. The empty space surrounded by perfluoroalkyl chains, available for inclusion of organic molecules, showed unique properties such as weak interaction between perfluoroalkyl chains and guest molecules. These modified layered materials can thus be used as adsorbents, matrices of photofunctional molecules, photochemical reaction media and so on.[25] Indeed, since fluorine-based surfactants are known to exhibit a distinct packing behavior comparing to those usually observed for analogous hydrocarbon surfactants,[26] interesting packing behavior should be obtained when perfluoroalkyl groups are combined with layered materials. Recently, Yui *et al.* have demonstrated that polyfluorinated surfactants of general formula $C_nF_{2n+1}CONH\text{-}(CH_2)_2\ N^+(CH_3)_2C_{16}H_{33}\ Br^-$ (CnF−S where n = 1, 2, 3, 4, 5, 6, 8, and 10) are able to intercalate in amounts exceeding the cation exchange capacity (CEC) of the clay. The C4F−S and C5F−S surfactants exhibited intercalation up to 480% of the CEC as a saturation adsorption limit. The surfactant molecules form a rigidly packed bilayer structure in the clay interlayer and are tilted at an angle of about 60° relative to the clay layer.[27]

Organoclays containing fluorosurfactants were also used as filler for the preparation of acrylic polymers nanocomposites by in situ intercalative photopolymerization.[28,29] Di Gianni *et al.* have used fluorinated ammonium salts containing a fluoroalkyl or a perfluoropolyether chain to prepare acrylic nanocomposites through photopolymerization. The clay modified by the fluoroalkyl surfactant exhibited a higher degree of intercalation leading to a transparent UV-cured polymer with better water adsorption properties.[30]

In this work, we were interested on utilization of new series of polymerizable quaternary ammonium surfactants bearing a perfluorocarbon chain and an acrylic polymerizable moiety as clay modifiers for the preparation of polystyrene−clay nancocomposites. The main objective of this work is to study the synergic effect of fluorine moiety and polymerizable function on the morphology and thermal properties of polystyrene (PS) nanocomposites. The combination of these two entities in the same structure should promote the exfoliation process and have a direct impact on the thermal properties of the final composites. The structures and the properties of the obtained composites were studied using Wide-angle X-ray diffraction measurements (WAXD), transmission electron microscopy (TEM), scanning electron microscopy (SEM) and thermal gravimetric analysis (TGA).

EXPERIMENTAL

Materials

Styrene was purchased from Sigma Aldrich and purified by washing with an aqueous solution of 5*M* NaOH to remove inhibitor followed by washing three times with deionized water then stored at −20°C. Surfmers F.n-l-m, H.8-11 and F.6-6-N-12 were synthesized as reported previously.[31] The sodium montmorillonite, Cloisite Na^+ (MMT), used in this study was kindly provided from Southern Clay Products, Inc. (USA). It has a cation exchange capacity of 92.6 mequiv/100 g of clay. 2,2'-azobis(isobutyronitrile) (AIBN), other organic chemicals and solvents were purchased from Sigma-Aldrich.

Organoclays and Nanocomposites Characterizations

Wide-angle X-ray diffraction measurements (WAXD) were carried out on the organoclay powders and on nanocomposites using a Bruker-D8 advance AXS, 40 KV, 40 mA (Cu K_α radiation; θ: 2–20°). The FT-IR measurements were performed using a Perkin Elmer™ FT-IR Paragon® instrument: the clay mineral powder was mixed with KBr, by pressing the mixture in vacuum; a disk was obtained and used as specimen. The wavenumbers are measured from 400 to 4000 cm^{-1}. Thermogravimetric analysis (TGA) was performed with a TGA7–Perkin Elmer instrument at a heating rate of 10°C/min in air from 25–900°C. Morphology of the composites was investigated by scanning electron microscopy (SEM) using a JOEL 6700F.

For TEM measurements, the specimens were embedded in Epoxy resin. Ultrathin 80 nm sections were cut with a Leica Ultracut S and observed in a JEOL JEM 1400 transmission electron microscope operating at 100 kV and equipped with a MORADA SIS camera. Gel Permeation Chromatography (GPC) analysis was carried with an isocratic pump Agilent 1200 series equipped with an autosampler Agilent 1200 Series and a refractometer detector Waters 2414. Calibrations were made

according to polystyrene standards with THF as an eluent. Samples were filtered through a PTFE 0.45-μm filter Acrodisc 13 mm prior to analysis.

Clay Modification

The ion exchange reactions of clay with ammonium surfactants were conducted as follow: 3 g of Cloisite Na^+ clay were suspended in 250 mL of distilled water and stirred at 700 rpm. A solution of 3 equivalents of surfmer or F.6-6-N-12 surfactant with regards to the cation exchange capacity (CEC) dissolved in 100 mL of water was slowly added under stirring . The resulted suspension was intensively stirred for 24 h at ambient temperature. The resulting dispersion is then filtered and extensively washed with water in order to remove the excess of unreacted surfactant. 0.1M solution of $AgNO_3$ was used to detect the presence of bromide counterions released in the filtrate. The washing was stopped if there is any precipitate formed after $AgNO_3$ addition. The final product was dried overnight under vacuum at 40°C then grounded into fine powder.

Reverse Ion Exchange

For the determination of molecular weights of the bounded PS chains in the PS/clay nanocomposites, 1 g of PSF.6-6-2MMT nanocomposite was dissolved in THF. The clay mineral was filtered then treated with 0.9 g of LiBr in THF. The mixture was refluxed during 48h. The released polymer was precipitated in methanol then dried and used for GPC measurements.

Synthesis of Polystyrene-Clay Nanocomposites

By using bulk polymerization, a series of Polystyrene-clay nanocomposites were prepared in a Schlenk tube. Briefly, 1 g of styrene monomer, various amounts (1, 5, 10 or 15 wt %) of organoclay (based on styrene weight) and 1wt % of AIBN initiator were mixed. The mixture was degassed with nitrogen three times then sonicated for 4 h in a cold water bath to ensure a good dispersion of the clay. The mixture was heated at 60°C for 24 h then 80°C for further 24 h. The obtained polymer was solubilized in a minimum quantity of chloroform, precipitated in methanol and dried to afford a white powder.

Solution polymerization was conducted in the same manner except that 2 mL of acetonitrile were added to the initial mixture before sonication.

RESULTS AND DISCUSSION

The use of clay as polymer filler for the preparation of nanocomposites requires the organic modification of clay with cationic surfactants to ensure compatibility of clay with polymer matrix. The cation exchange process was extensively used to introduce organic compounds such as surfactants, pollutants and dyes within clay galleries leading to the increase of interlayer distance between clay platelets as well as the modification of the polarity of the clay.

In this context, we designed in this study a series of fluorine based reactive surfactants which combine in their structure a fluorinated chain and an acrylic polymerizable function, as shown in Scheme 1. The nomenclature chosen for these fluorinated products is F.n-l-m where n is the number of carbon atoms in the fluorocarbon tail, l is the number of carbon atoms in the spacer linking the fluorinated chain to the ammonium head and m is the number of carbon atoms between the polymerizable acrylate moiety and the ammonium head.

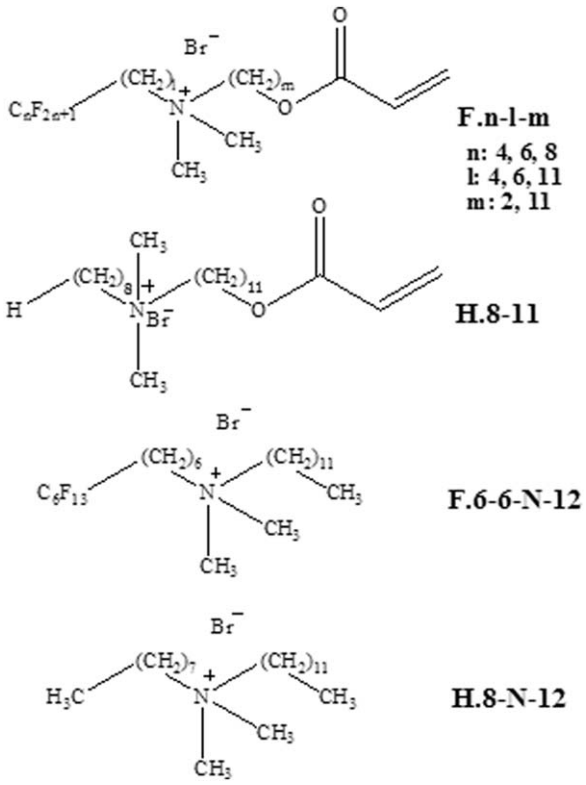

Scheme 1. Chemical structure of investigated surfactants.

The selection of these structures allows us to determine the effect of different structural parameters on the morphology and properties of the corresponding nanocomposites such as: the length of the fluorinated chain, the length of the spacer linking the fluorinated chain to the ammonium head and the ammonium group to the acrylic function.

Three reference molecules were also prepared: a hydrocarbon surfmer (H.8-11) which has an analogous structure as the fluorinated surfmers F.n-l-m and particularly F.4-4-11 and non polymerizable hydrocarbon and fluorinated surfactants noted H.8-N-12 and F.6-6-N-12 respectively. These surfactants were used to investigate the impact of the fluorine moiety and the polymerizable group on the resulting nanocomposites.

Modification of Clay with Surfactants

A preliminary study to determine the optimum conditions to prepare the organoclays was conducted. The polymerizable surfactants F.6-6-2 and H.8-11 surfmers were used to modify the pristine clay cloisite Na^+ (MMT). Three parameters were varied: a) the concentration of surfactant: 1.5 or 3 equivalents regarding the clay cation exchange capacity (CEC), b) the stirring time : 3h, 6h, 24h and 48h and c) suspension temperature: ambient and 50°C.

The resulting modified MMT clays were first characterized by FTIR to confirm the presence of surfactant molecules in the clay. FTIR spectra of F.6-6-2 modified clay (F.6-6-2MMT),

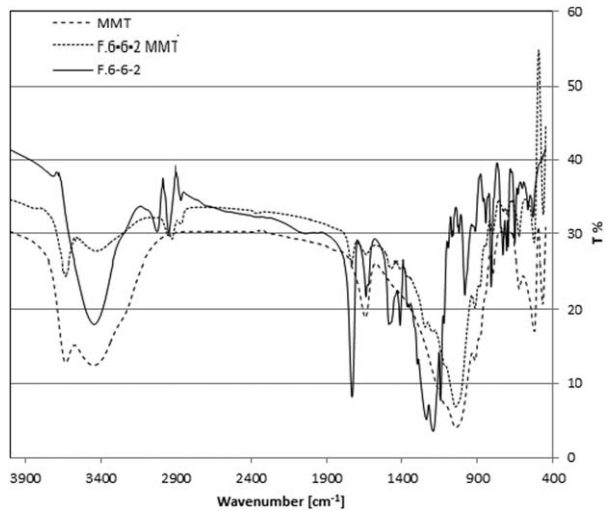

Figure 1. FTIR spectra of the sodium montmorillonite (MMT clay), the surfmer F.6-6-2 and the modified clay F.6-6-2MMT.

montmorillonite clay MMT and F.6-6-2 surfmer are reported in Figure 1. It is noticed that the vibration bands of the principal functions related to MMT and surfmer are presents in the organoclay spectrum. The intense peaks at 1057, 466 and 522 cm^{-1} are related to stretching and bending vibrations of Si-O. The band at 1115 cm^{-1} is due to out-of-plane stretching of Si-O of clay. The large stretching bands at 1665 and 3634 cm^{-1} are attributable to hydrogen-bonded water related to OH bending,

We noted an appreciable decreasing of intensity of these bands in the organoclay in comparison with the virgin cloisite Na^+. The same behavior was reported by Vazquez *et al.*[32] The peak at 1738 cm^{-1}, characteristic of carbonyl stretching of the acrylate function, provides the proof that surfmer is incorporated in the organoclay either intercalated inside the platelets or at the physisorbed state. This peak is slightly shifted to higher wavelength in comparison with surfmer probably due to the interaction between the surfactant carbonyl function and the clay surface through hydrogen bonding with hydroxyl groups localized at the clay outermost surface.

The peak at 1296 cm^{-1} is due to stretching vibration of C-F bond of perfluoroalkyl chains. The symmetric and asymmetric stretching of C-H bands of hydrocarbon spacers were observed at 2851 cm^{-1} and 2923 cm^{-1}. All organoclays spectra exhibit the same characteristic peaks.

Thermogravimetric analysis was used to estimate the quantity of surfactants incorporated in monomorillonite clay and consequently the efficiency of cation exchange reaction. On the basis of CEC value, the degree of modification (X) was calculated according to the following equation:[33]

$$X = \frac{[\text{residual weight before modification}] - [\text{residual weight after modification}]}{\text{molar weight of surfacant}} \cdot \frac{1000}{CEC} \cdot 100$$

Table I lists the degree of modification of F.6-6-2MMT and H.8-11MMT at various operating conditions. As clearly noticed, the increase of stirring time favors the incorporation of surfactants molecules as the organic content increases from 18 to 58% and from 29 to 60% for F.6-6-2MMT and H.8-11MMT dispersions respectively when stirring time increases from 6h to 48h. However, the increase of the surfactant concentration from 1.5 to 3 equivalents permitted to accede to the best modification levels in shorter time (24h) at room temperature. The dispersion temperature was also found to be a critical parameter: higher temperature promote exchange process particularly for the fluorinated surfmer.

Accordingly, we have opted the latter conditions ([surfactant] = 3eq/CEC, 25°C, 24 h) to prepare the following dispersions. We preferred to avoid heating to prevent side polymerization reactions during surfactant intercalations.

The amount of ion exchanged surfmers and surfactants in sodium montmorillonite were measured and listed in Table II. Two molar masses were used for each surfactant to calculate these values: with and without bromide ions. In fact, it was reported that depending on surfactant concentration, the ammonium ions adsorb on the cation-exchangeable sites without or with the bromide counter anions. In the first case, the anionic sites of the clay surface are electrically neutralized by the ammonium ions leading to intercalation and removing of sodium bromide from the interlayer. In the second case, the surfactants are incorporated as neutral molecules to the already neutralized interlayer space.[23]

The two amounts of ion exchanged surfmers agree defining an intercalating range of each surfactant in the clay. The obtained results indicate that 59–73% (with Br ion) and 71.5–81.5% (without Br ion) of the available site (CEC) were exchanged which is comparable with the behavior of similar reactive surfactants towards mineral clays described in the literature.[20,34,35]

WAXD analyses were used to measure the interlayer distance (d) after ion exchange reaction. The sodium montmorillonite spectra showed a reflection peak at $2\theta = 7.21°$ corresponding to $d_{001} = 12.2$ Å. This value is comparable with similar hydrated clays reported in the literature.[36]

After clay modification, we observed for all the prepared organoclays, an appreciable increase of basal d spacing (Table II) confirming, as for TGA analysis, that the intercalation has really occurred. In Figure 2(a) are given, as example, WAXD spectra of Cloiste Na^+ and F.6-6-2MMT organoclay.

The nonpolymerizable surfactants H.8-N-12 and F.6-6-N-12 gave the higher sheet expansion corresponding to d_{001} of 24.4 and 25.1 Å respectively. However, in the both cases, two supplementary peaks were observed : the first one at 11.2 and 10.7 Å for H.8-N-12 and F.6-6-N-12 surfactants respectively

Table I. Effect of Operating Conditions on the Degree of Modification of MMT Clay (Stirring Speed 700 rpm)

Surfmers	[Surfmer]/ CEC	Temperature (°C)	Stirring time (h)	Degree of modification (%)
F.6-6-2	1.5 eq	25	6	18.0
	1.5 eq	25	24	36.9
	1.5 eq	25	48	57.6
	1.5 eq	50	3	53.6
	3 eq	25	24	61.8
H.8-11	1.5 eq	25	6	28.9
	1.5 eq	25	24	37.5
	1.5 eq	25	48	60.5
	1.5 eq	50	3	51.9
	3 eq	25	24	67.5

corresponding probably to unmodified clay and the second at 14.4 Å and 15.4 Å (majority) indicating that another layer structure population coexist in the sample [Figure 2(b)].

On the other hand, the hydrocarbon surfmer H.8-11 induce a greater increase of basal spacing (d ~ 21.9 Å) as compared to fluorinated surfmers with similar structure. The impact of the length of fluorinated chain and hydrocarbon spacer is more complex. It clearly appears that the lengthening of the hydrocarbon spacers l and m let an increase of the interlayer distance (Figure 3). In fact, d_{001} value varied from 16.8 Å to 19.4 Å for clay modified with F.6-6-2 and F.6-6-11 respectively (m = 2 and 11). Likewise, a gradual increase of d in the order of 14.9 Å, 16.8 Å and 20.2 Å for l = 4, 6 and 11 respectively was noticed.

The effect of fluorine chain length is not linear. The shorter, C_4F_9, fluorinated chain leads to the higher d value.

Previous study suggested that depending on basal spacing value, it was possible to predict the orientation of ammonium surfactants within clay layers.[37] Monolayer parallel orientation of surfactant molecules is obtained for d_{001} of 1.4 nm, a lateral bilayer for d_{001} of 1.8 nm, a pseudotrimolecular layer d_{001} of 2.3 nm and an inclined paraffin structure for d_{001} of 4.6 nm.

Based on these results, and assuming that our surfmers behave as classic ammonium surfactants in clay, we can expect that F.6-4-2, F.6-6-2 and F.6-6-N-12 are arranged in a monolayer, H.8-N-12 and a small population of F.6-6-N-12 are oriented in pseudotrimolecular layer while the others surfmers form a bilayer.

In order to have further information about the orientation of surfactant molecules, we calculated the optimized structures using PM3 (parameterized model number 3) method. Different parameters were thus determined: L_1: the length of the side opposite to the triangle, L_2: the length of the fluorinated chain, L_3: the length of the hydrocarbon chain including the ammonium head and α: the banding angle between the two arms of surfactant molecule.

An example of the optimized structure of surfmer F.6-6-2 molecule is presented in Figure 4(a). A triangular structure with a binding at the junction fluorinated chain-hydrocarbon chain was obtained for all studied surfactants except for compound F.6.6-11 where the structure bends in two positions: at fluorinated-hydrocarbon junction and in the hydrocarbon spacer between the ammonium head and the acrylic function at C3 carbon starting from the ammonium [Figure 4(b)].

The resulting geometric parameters of surfmer and surfactant molecules are listed in Table III.

On the other hand, clearance spaces were calculated by subtracting the intrinsic clay layer thickness (9.6 Å)[28] from the experimental layer distance obtained by WAXD analysis. The resulting values are close to L_2 which is in favor of a parallel alignment of surfactant molecules to the clay layer. The clearance spaces and L_2 values are particularly close for F.6-4-2, F.6-6-2 and F.6-6-N-12 surfactants suggesting a monolayer arrangement.

The clearance spaces of the others surfactants are greater than L_2 and lower than L_1 and L_3 values thus a multilayer arrangement (bilayer, peseudotrilayer.) will be more probable. In this case, surfactants molecules could also be inclined relative to clay layer (Scheme 2).

Polystyrene–Clay Nanocomposites

The modified clays were added to styrene at amounts of 1%, 5%, 10% and 15 wt % then sonicated for 4 hours to unsure a good dispersion of clay pallets in styrene monomer. The polymerization was performed in situ in acetonitrile solution or in bulk. Polystyrene devoid of clay was also prepared under the same polymerization conditions as a reference standard.

FTIR spectra of nanocomposites obtained by bulk or solution polymerization are almost the same and contain the characteristic absorption bands of the different constituents i.e.

Table II. Amount of Surfactants Incorporated into the Cloisite Na^+ and Interlayer Distance d_{001} of Corresponding Organoclays

Material	Degree of modification (%) with Br ion (without Br ion)	$2\theta°$	d_{001} (A°)
MMT		7.21	12.2
F.4-6-2MMT	66.2 (76.3)	4.11	21.5
F.6-4-2MMT	59.3 (79.0)	5.92	14.9
F.6-6-2MMT	61.8 (79.6)	5.24	16.8
F.6-11-2MMT	72.7 (81.5)	4.36	20.2
F.6-6-11MMT	60.9 (76.5)	4.54	19.4
F.8-6-2MMT	68.8 (81.8)	4.87	18.2
H.8-11MMT	67.5 (80.8)	4.03	21.9
F.6-6-N-12MMT	63.3 (71.5)	8.22	10.7
		5.73	15.4 (majority)
		3.51	25.1
H.8-N-12 MMT	69.9 (72.1)	3.61	24.4 (majority)
		6.10	14.4
		7.90	11.2

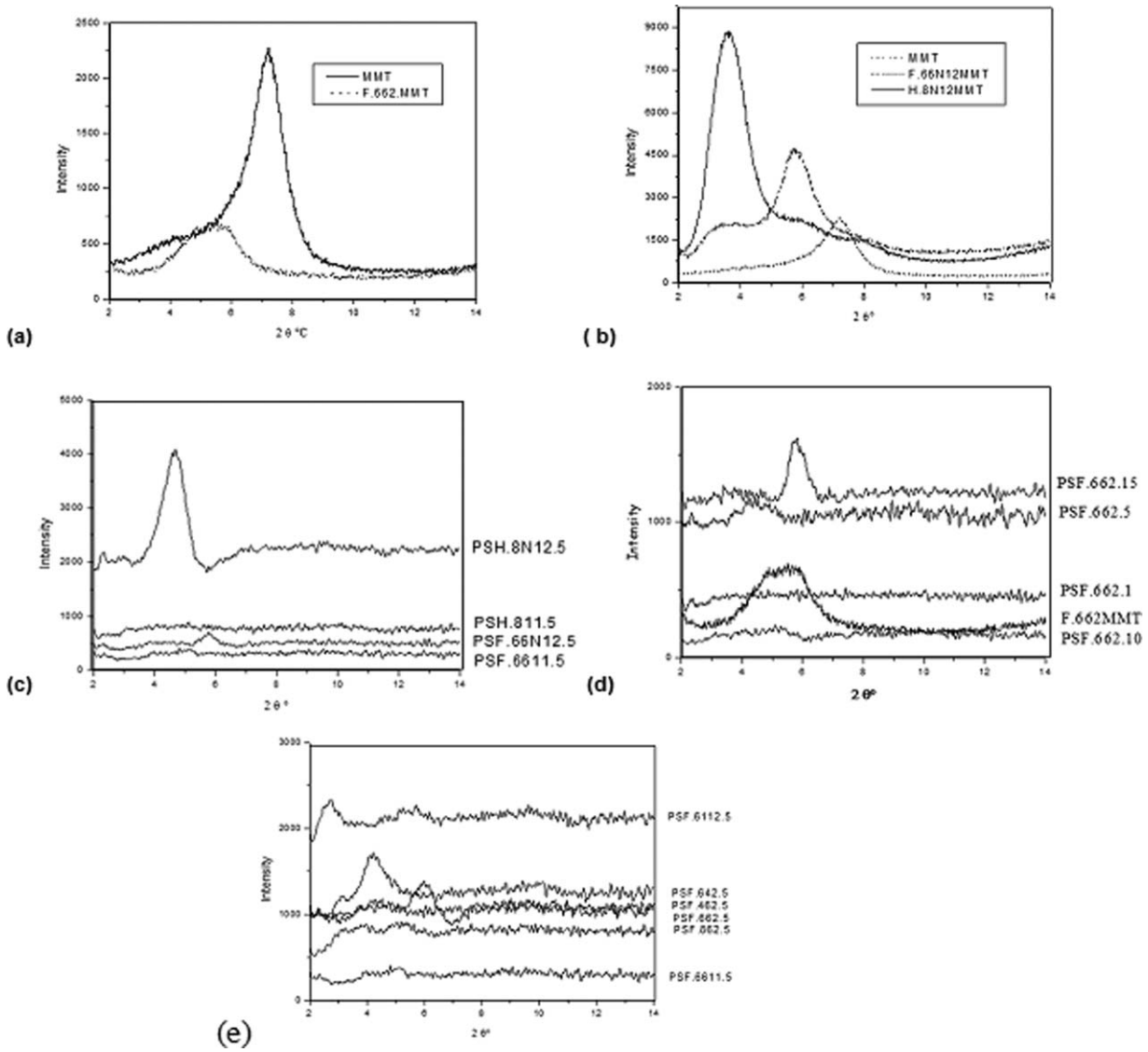

Figure 2. WAXD spectra of: (a) MMT clay and F.6-6-2MMT organoclay (b) F.6-6-N-12MMT and H.8.N-12MMT organoclays (c) nanocomposites based on fluorinated and hydrocarbonated surfmers and surfactants, (d) nanocomposites PSF.6-6-2 (1, 5, 10, and 15%), (e) nanocomposites PSF.n-l-m ($n = 4,6,8$; $l = 4,6,11$; $m = 2,11$).

polystyrene, clay and surfmers. The attribution of the main absorption bands of polystyrene – F.6-6-2 5% nanocomposites are presented as an example in Table IV.

WAXD and TEM analysis were used to determine the morphology of prepared nanocomposites, to establish the effect of the modulated parameters i.e. polymerization method and surfactant structural parameters (n, l, m and the polymerizable group) on the extent of the organoclay dispersion within polystyrene. The obtained results are summarized in Table V.

Comparison of XRD analysis of PS-F.6-6-2MMT 5% and 10% composites prepared by bulk and solution polymerization showed that the latter mode of polymerization promotes the formation of intercalated structures. This is in good agreements with earlier literature data.[38]

The WAXD patterns of polystyrene nanocomposites containing 5 wt % of organoclays based on F.6-6-2, H.8-11, F.6-6-N-12 and H.8-N-12 surfmers [Figure 2(c)] indicated clearly the effect of fluorine and polymerizable moieties on the morphology of the corresponding nanocomposites. Hydrocarbon surfmer H.8-11 enables the complete exfoliation of clay pallets as compared to the nonpolymerizable surfactant H.8-N-12 which exhibited an intercalated structure with an intense peak at d value of 18.5 Å. Low intensity broad peaks were observed at 37.7 Å and 51.5 Å due probably to the presence of occasional small tactoids.

The same positive impact of acrylic function for the elaboration of exfoliated structures was observed in fluorinated series (F.6-6-11 and F.6-6-N-12). However, the XRD spectra indicate that partial exfoliation occurred even for non polymerizable surfactant F.6-6-N-12. Only a small broad peak at 15.1 Å was observed in its spectra suggesting that a residual quantity of corresponding organoclay (d_{001}= 15.4 Å) still in the order intercalated state.

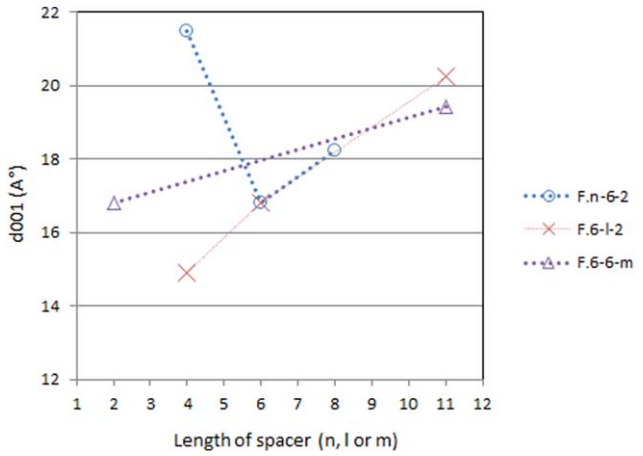

Figure 3. Evolution of the organoclay interlayer distance based on fluorinated surfactant structural parameters *n, l,* and *m.* [Color figure can be viewed in the online issue, which is available at wileyonlinelibrary.com.]

These results suggest that fluorine moiety acts favorably for the establishment of well dispersed systems probably due to it dispersive known effect. Based on these data, it is possible to establish a classification of structures relative to their increasing promoting exfoliation effect: hydrocarbon surfactant < hydrocarbon surfmer < fluorine surfactant < fluorine surfmer.

The effect of organoclays quantity incorportated in nanocomposites was also considered. Polystyrene – F.6-6-2MMT systems have been taken as models [Figure 2(d)]. While 1 and 10% nanocomposites show exfoliated structure verified by TEM images [Figure 5(a)] and the absence of diffraction peaks in WAXD, the 5% composites exhibits a large broad peak at 25.1 Å attributed to either a partial exfoliation or a disordering in the clay tactoids.

TEM analysis supports the partially exfoliated structure [Figure 5(b)]. The existence of some agglomerates can be seen indicating the heterogeneous distribution of clay layers in the polystyrene matrix.

The 15% nanocomposite has an intercalated morphology confirmed by TEM [Figure 5(c)] and WAXD analysis. A basal spacing of 15.0 Å was noted for this composite slightly lower than

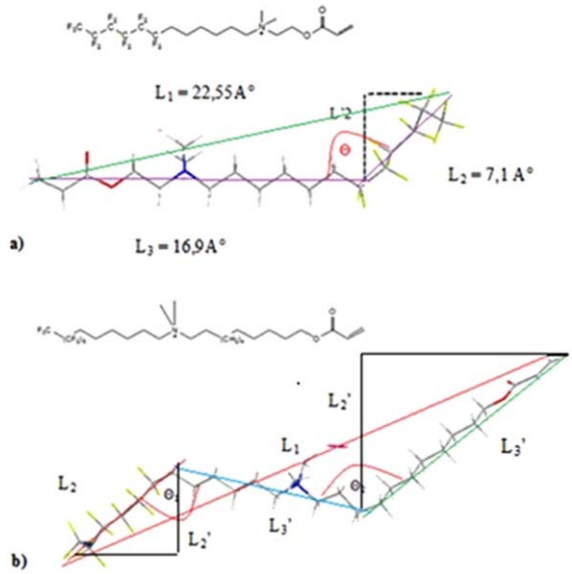

Figure 4. Optimized molecular structure of surfmers (a) F.6-6-2 and (b) F.6-6-11. [Color figure can be viewed in the online issue, which is available at wileyonlinelibrary.com.]

that obtained for the corresponding organoclay F.6-6-2MMT (d = 16.8 Å). This decrease trend of basal spacing has been already described for surfmer based nanocomposites. The growing styrene chain reacted with some surfmer molecules intercalated in clay gallery leading to a pinning of the clay layers and thus the reduction of basal spacing while maintaining the clay order.[35,39,40]

The design of surfactant could also be a key parameter to achieve well exfoliated nanocomposites. In the past, Simon *et al.* have described some structural parameters to take into account for this purpose: the location of ammonium head which should be adjacent to polymerizable group, the presence of the polymerizable group and the lengthening of the alkyl chain.[35]

The comparison of WAXD spectra of 5% nanocomposites prepared from surfmers with similar structure and bearing different fluorine chain length F.4-6-2, F.6-6-2 and F.8-6-2

Table III. Molecular Geometry Parameters of Fluorinated and Hydrocarbon Surfmers and Surfactants

	L_1 (A°)	L_2 (A°)	L'_2 (A°)	L_3 (A°)	Θ (°)	Clearance space (A°)
F.4-6-2 F.6-4-2	16.8 13.4	4.8	2.8	16.8	107.9	11.9
		5.4	5.2	14.6	106	5.3
F.6-6-2	21.6	6.3	5.3	17.0	117.8	7.2
F.6-11-2	23.1	4.8	3.5	21.7	105	10.6
F.6-6-11	31.3	6.9	5.5	L_3 16.2	Θ_1 128	9.8
			14.6	L_3' 14.8	Θ_2 113.3	
F.8-6-2	21.6	6.3	5.1	18.2	114.5	8.6
H.8-11	25.7	14.7	9.9	14.3	119.1	12.3
F.6-6-N-12	28.9	6.7	6.1	24.9	128.1	5.8; 15.5
H.8-N-12	25.5	10.8	6.0	15.7	170.7	14.8

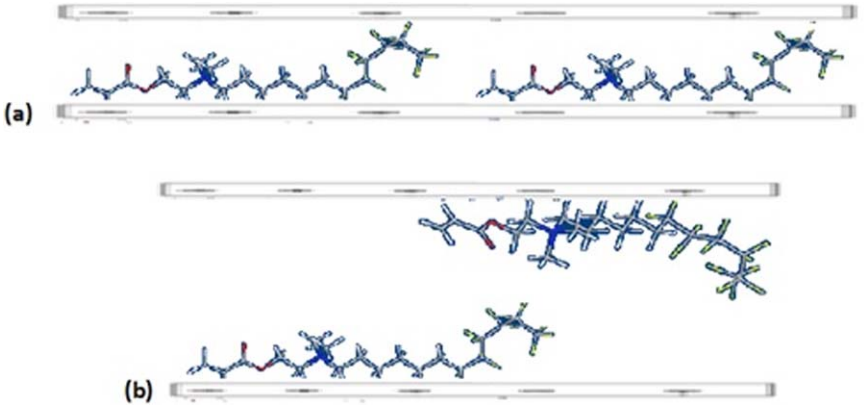

Scheme 2. Possible orientation of surfactant within clay layers: (a) Monolayer, (b) bilayer structure. [Color figure can be viewed in the online issue, which is available at wileyonlinelibrary.com.]

Table IV. Characteristic IR Bands of PS and PSF.6-6-2 5% Nanocomposites

	Wavenumber (cm^{-1})		
Functional groups	PS	PSF.6-6-2 5% (bulk)	PSF.6-6-2 5% (solution)
Al—O		614	631
Si—O		459, 526, 1031	462, 522, 1033
$-CH_2$	1441, 1489	1461-1491	1450, 1481
C=C	1762-1936	1725-1966	1731-1947
C—O		1117, 1200	1217, 1247
C=O		1638, 1733	1653, 1718
C—F		539, 568	694, 740
C—H	2846, 2930	2940, 3044	2851, 2923
O—H		1668, 3453, 3655	1665, 3476, 3618
Ar—H	3022, 3061, 3084	3017, 3032, 3063	1665, 3446, 3634

Table V. Morphology and Basal *d* Spacing of PS-Clay Composites

Material	Clay loading (%)	Polymerization[a]	Nanocomposite morphology	*d* (A°)
MMT				12.3
PSF.4-6-2	5	B	Intercalated	14.4
PSF.6-4-2	5	B	Intercalated	20.6
PSF.6-6-2	1	b	Exfoliated	–
	5	b	Partially exfoliated Intercalated	
	5	s	Exfoliated	25.4
	10	b	Intercalated Intercalated	–
	10	s		15.1
	15	b		15.0
PSF.6-11-2	5	B	Partially exfoliated	15.8
PSF.6-6-11	5	B	Exfoliated	–
PSF.8-6-2	5	B	Partially exfoliated	–
PSH.8-11	5	b	Exfoliated	–
	10	b	Exfoliated	–
PSF.6-6-N-12	5	B	Partially exfoliated	15.1
PSH.8-N-12	5	B	Intercalated	18.5

[a] Nanocomposites prepared by: b, bulk; s, solution.

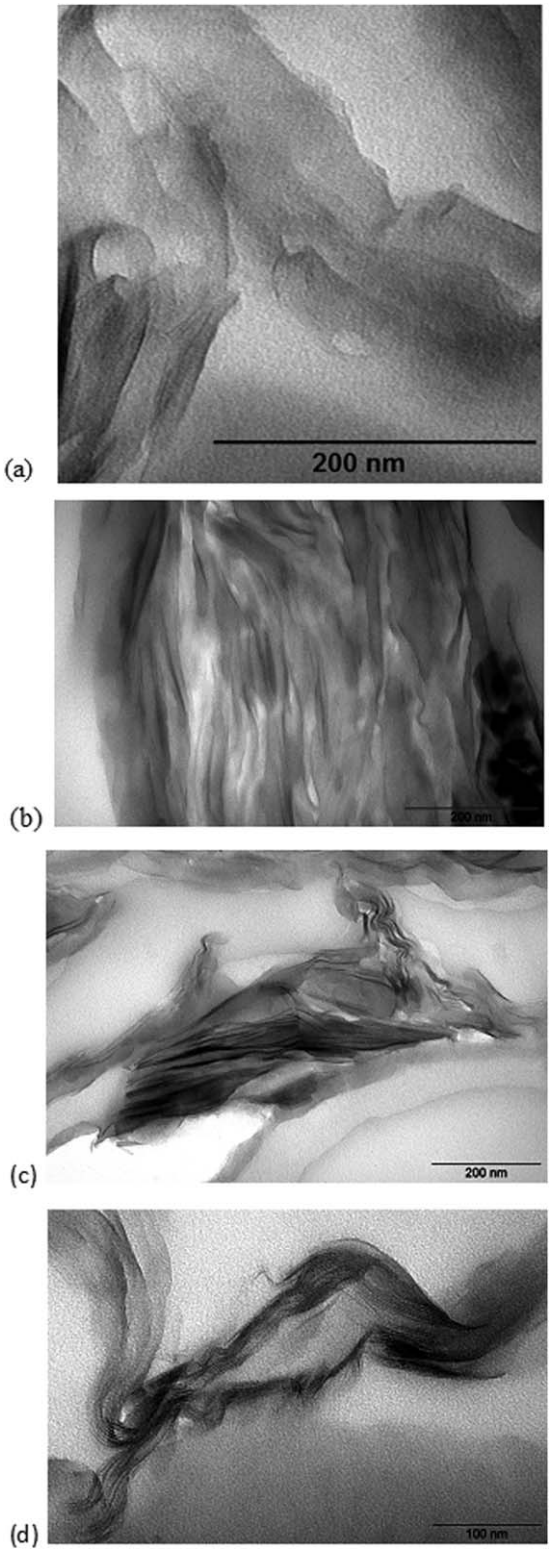

Figure 5. TEM images of nanocomposites (a) PSF.6-6-2 1%, (b) PSF.6-6-2 5%, (c) PSF.6-6-2 15% (d) PSF.6-4-2 5%.

[Figure 2(e)] indicates that surfactant with shorter fluorine chain led to intercalated structure while longer fluorine homologous allow the formation of better dispersed exfoliated nanocomposites.

The same trend was observed for the hydrocarbon spacer (l) connecting the fluorine chain with the ammonium head. While nanocomposite based on F-6-4-2 surfmer has an intercalated morphology with a basal spacing at 20.59 Å which corroborates TEM images [Figure 5(d)], surfmers with longer spacer (F.6-6-2, F.6–11-2) present exfoliated structures. For this latter system, small peak at $2\theta = 2.68$ indicate the presence of some tactoid assemblies.

The second spacer m present between the ammonium head and the acrylic function acts in the same manner: the lengthening of m (from 2 to 11) conduct to exfoliated morphology [Figure 2(e)].

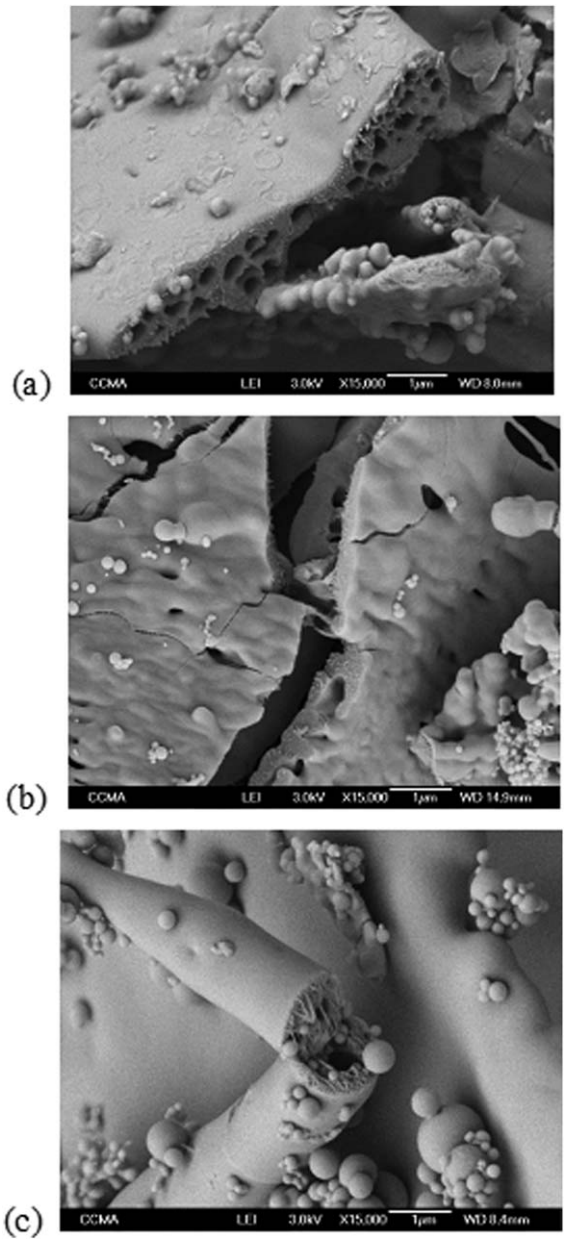

Figure 6. SEM micrographs of nanocomposites (a) PSF.6-6-2 1%, (b) PSF.6-6-2 5%, (c) PSF.6-6-2 15%.

Table VI. Thermal Stability of Polystyrene Nanocomposites Clay

Material	Clay loading (%)	T20	T50	Experimental char (%)	Theoretical[a] Char (%)
PS		347	380	1.29	
PSF.4-6-2	5	386	425	7.78	4.51
PSF.6-4-2	5	391	430	8.98	4.60
PSF.6-6-2	1	353	390	1.61	1.97
	5	393	431.5	9.74	4.71
	5[a]	379	422.3	7.53	4.71
	10	408	436.5	17.99	8.13
	15	398	432	22.81	11.55
PSF.6-11-2	5	402	432	5.22	3.90
PSF.6-6-11	5	414	445	7.01	3.94
PSF.8-6-2	5	394	432.5	8.98	4.46
PSH.8-11	5	366	400	9.19	2.83
	5[a]	364	398.5	6.33	2.83
PSF.6-6-N-12	5	357	392	4.46	4.18

[a] Nanocomposite prepared by solution polymerization.
[a] Theroretical char = [(100- % organic content of organoclay calculated by TGA) (quantity of organoclay)/100] +1.29. The % organic content of organoclay = mass loss due to physisorbed water at 170°C – mass loss at 700°C.

SEM micrographs of nanocomposites loaded with 1%, 5% and 15% of F.6-6-2MMT organoclay showed that the increase of the quantity of nanofiller in polystyrene matrix conducts to nanocomposites having more irregular and porous aspects (Figure 6).

All samples present many tortuous crack propagation lines leading to a porous structure upon failure. This is in agreement with earlier observation of Yilmazer and Ozden for polystyrene – clay nanocomposites prepared by in situ polymerization. These nonlinear cracks will have a direct impact on the strength of the material: more the tortuous cracks are formed during the fracture process; more energy should be absorbed to break the material.[41,42]

Thermal stability of the nanocomposites was studied by thermogravimetric analysis. Data summarized in Table VI show clearly the enhancement of thermal stability of polystyrene upon the addition of 5 wt % of organoclay. T20, the temperature at which the nanocomposites loses 20% of the initial mass, increases from 10 to 67°C comparing to neat polystyrene while the T50 are improved by 12 to 65°C. The enhancement in thermal stability is however independent of polymerization conditions (bulk or in solution). The clay being an inorganic material, it has a high thermal stability and great barrier properties, which can act as an insulator to prevent the propagation of heat and thus limit the decomposition of the nanocomposites.

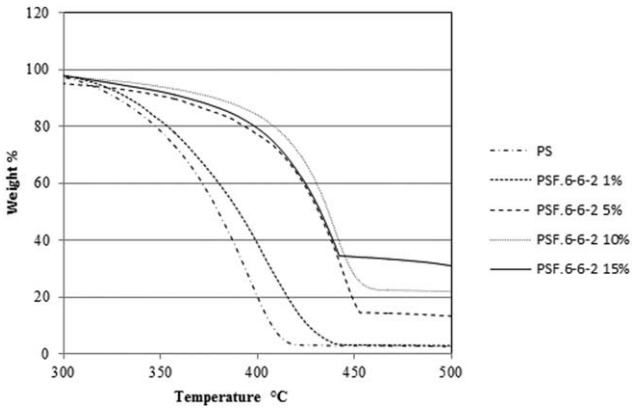

Figure 7. TGA curves of PSF.6-6-2 nanocomposite with different clay loadings.

The fluorinated surfmers-based nanocomposites are more stable than PS-hydrocarbon surfmer (H.8-11) composite which is itself more stable than the nonpolymerizable surfactant (F.6-6-N-12) based composite. It seems that introducing a fluorinated chain and a polymerizable function on the surfactant structure induces a synergic effect that favors positively the nanocomposite thermal stability.

The experimental chars of clay composites calculated as the residues obtained at 700°C are higher than the experimental values obtained from the organic content of organoclay calculated

Table VII. GPC Characterization of Polystyrene Nanocomposites

Nanocomposites	M_p (g/mol)	M_n (g/mol)	M_w (g/mol)	I_p (M_n/M_w)
PS	186,200	111,100	227,800	2.05
PSF.6-6-2 1%	69,860	52,310	189,100	3.62
PSF.6-6-2 5%	55,840	38,660	177,100	4.58
PSF.6-6-2 5% (bounded)	56,510	38,150	142,400	3.73
PSF.6-6-2 10%	59,940	43,830	131,300	2.99
PSF.6-6-2 15%	52,330	30,430	131,200	4.31

previously by TGA and the residual char of virgin polystyrene prepared in the same condition calculated by TGA. This tendency could be attributed to the accumulation of carbonaceous silicate char at the surface of polymer that acts as a heat and mass transfer barrier.[39] These materials can potentially be used as fire-retardancy materials.

Figure 7 shows the effect of the clay loading on the thermal stability of nanocomposites prepared from F.6-6-2MMT organoclay. The addition of only 1 wt % of organoclay lead to an improvement of T20 and T50 by 6 and 10°C respectively in comparison with pristine polystyrene. A thermal stability threshold is reached at 10 wt % corresponding to an increase of the T20 and T50 of the order of 61°C and 57°C respectively. These results are opposite to those reported by Samakande *et al.*[43] who reported a slight improvement in thermal stability with increasing of clay loading for polystyrene clay nanocomposite.

Another important parameter that has been studied is the effect of the surfactant design, i.e. the length of the fluorinated chain and the hydrocarbon spacers, on the thermal behavior of the nanocomposites. The fluorine length chain has a low effect on the thermal degradation of the nanocomposites. Surfmer with short fluorine chain C_4F_9 exhibits slightly lower T20 and T50 values which could be due to the intercalated morphology of this composite. This result agree with data reported for polystyrene/clay nanocomposites where exfoliated morphologies tends to have better thermal properties relative to the intercalated ones due to the better dispersion of clay platelets in the exfoliated nanocomposites.[22]

The lengthening of the hydrocarbonated spacer l present between the fluorine chain and the ammonium head has a little effect on degradation profile of the corresponding nanocomposites: the T20 is increased by 10°C for F.6-11-2 surfmer comparing to F.6-4-2 homologous while the T50 remains unchanged. The second spacer m has a more pronounced impact since the T20 and T50 are increased by 21°C and 13.5°C respectively for m =11. This can also be correlated to the exfoliated morphology of F.6-6-11MMT organoclay determined previously by WAXD and TEM analysis.

Finally, the molecular weights of the unbounded PS chains in the PS/clay nanocomposites were calculated by GPC analysis. Results summarized in Table VII show that the molecular weight are relatively high but are lower and more disperse than that of virgin polystyrene prepared in the same conditions. With increasing clay loading, the MW decreases which is consistent with earlier results reported in literature.[44] The presence of dispersed clay platelets on styrene matrix could enhance the viscosity of the medium and therefore hindered the diffusion of monomer molecules and free radicals leading increases chain transfer or termination reactions.

The bounded polystyrene of PSF.6-6-2 5% nanocomposite was recovered by reverse ion exchange. The number and weight average molecular weights of clay-attached polystyrene chains are close to that of the freely dispersed ones.

Since we have shown in a previous work the ability of these studied surfmers to copolymerize with styrene,[45] we can conclude that the structural and thermal modification observed for the corresponding nanocomposites is a result of the copolymerization reaction between surfmer molecules present in clay gallery and styrene molecules diffusing into the clay interlayer spacing leading to substantial movement of clay platelets.

CONCLUSIONS

Hybrid hydrocarbon/fluorocarbon ammonium type surfactant monomers (surfmers) of the general formula $R_F(CH_2)_lN(CH_3)_2(CH_2)_mOCOCH{=}CH_2$ with ($R_F = C_4F_9$, C_6F_{13}, C_8F_{17}, l = 4, 6, 11, and m = 2–11) were intercalated in monmorillonite clay. The resulting organoclays were used as fillers to prepare polystyrene nanocomposites through in situ free radical polymerization.

Structural and thermal characterizations of these materials enabled to highlight the effect of structural design of surfactant on the morphology and the thermal degradation of the resulting nanocomposites. A synergic effect of the introduction of a fluorine tail and a polymerizable function on the surfactant structure allowed the obtaining of well exfoliated nanocomposites with improved thermal stability. The main effect responsible of exfoliation is the combination of the dispersive effect of fluorine atoms and the extensive movement of the clay layers resulting from the copolymerization reaction of acrylic function of surfmer molecules present inside the clay galleries with styrene.

The lengthening of the hydrocarbonated spacers connecting the ammonium head to the fluorinated tail or the acrylic function acted also favorably for the achievement of well exfoliated structures. A direct impact of the morphology of the nanocomposites on their thermal behavior was noted. Exfoliated nanocomposites exhibit better thermal stability comparing to pristine polystyrene and could potentially act as fire-retardancy materials.

ACKNOWLEDGMENTS

This work was supported by an Averroes doctoral grant. The authors thank J.P. Laugier and S. Pagnotta for the SEM and TEM images that were performed at the CCMA (Centre Commun de Microscopie Appliquée) of the Université de Nice Sophia Antipolis.

REFERENCES

1. Li, G. L.; Zheng, L. Q.; Xiao, JX. *J. Fluorine Chem.* **2009**, *130*, 674.
2. Erol, I. *J. Fluorine Chem.* **2008**, *129*, 613.
3. Sacher, F. *Prog. Surf. Sci.* **1994**, *47*, 273.
4. Pu, F. R.; Williams, R . L.; Markkula, T. K.; Hunt, J. A. *Biomaterials* **2002**, *23*, 2411.
5. Lina, M. J.; Dessaint, A. EP Pat. CAN 108: 22421,1987, No. 225026.
6. Casazza, E.; Mariani, A.; Ricco, L.; Russo, S. *Polymer* **2002**, *43*, 1207.
7. Saidi, S.; Guittard, F.; Geribaldi, S. FR Pat. 2003207 **2003**.
8. Satoh, K.; Nakazumi, H. *J. Sol-Gel Sci. Technol.* **2003**, *27*, 327.
9. Chuang, S. W.; Hsu, SL-C.; Liu, Y-H. *J. Membrane Sci.* **2007**, *15*, 353.

10. Roghani-Mamaqani, H.; Haddadi-Asl, V.; Najafi, M.; Salami-Kalajahi, M. *J. Appl. Polym. Sci.* **2011**, *120*, 1431.
11. Panwar, A.; Choudhary, V.; Sharma, D. K. *J. Reinfor. Plast. Comp.* **2011**, *30*, 446.
12. Uthirakumar, P.; Song, M. K.; Nah, C.; Lee, Y. S. *J. Eur. Polym.* **2005**, *41*, 211.
13. Uhl, F. M.; Wilkie, C. A. *Polym. Degrad. Stab.* **2002**, *76*, 111.
14. Vyazovkin, S.; Dranca, I.; Fan, X.; Advincula, R. *J. Phys. Chem. B* **2004**, *108*, 11672.
15. Qin, X.; Wu, Y.; Wang, K.; Tan, H.; Nie, J. *Appl. Clay Sci.* **2009**, *45*, 133.
16. Bottino, F. A.; Fabbri, E.; Fragala, I. L.; Malandrino, G.; Orestano, A.; Pilati, F.; Pollicin, A. *Macromol. Rapid Commun.* **2003**, *24*, 1079.
17. Sain, S.; Khatua, B. B. *Macromol. Res.* **2011**, *19*, 44.
18. Qutubuddin, S.; Fu, X. A.; Tajuddin, Y. *Polym. Bull.* **2002**, *48*, 143.
19. Uthirakuma, P.; Nahm, K. S.; Hahn, Y. B.; Lee, Y. S. *Eur. Polym. J.* **2004**, *40*, 2437.
20. Fu, X.; Qutubuddin, S. *Polymer* **2001**, *42*, 807.
21. Zeng, C.; Lee, L. *Macromolecules* **2001**, *34*, 4098.
22. Zhang, W. A.; Chen, D. Z.; Xu, H. Y.; Shen, X. F.; Fang, Y. E. *Eur. Polym. J.* **2003**, *39*, 2323.
23. Yui, T.; Yoshida, H.; Tachibana, H.; Tryk, D. A.; Inoue, H. *Langmuir* **2002**, *18*, 891.
24. Yui, T.; Uppili, S. R.; Shimada, T.; Tryk, D. A.; Yoshida, H.; Inoue, H. *Langmuir* **2002**, *18*, 4232.
25. Matsuo, Y. *J. Fluorine Chem.* **2007**, *128*, 336.
26. Oumar, M.; Taffin de Givenchy, E.; Dieng, S. Y.; Amigoni, S.; Guittard, F. *Langmuir* **2011**, *27*, 1668.
27. Yui, T.; Fujii, S.; Matsubara, K.; Sasai, R.; Tachibana, H.; Yoshida, H.; Takagi, K.; Inoue, H. *Langmuir* **2013**, *29*, 10705.
28. Benfarhi, S.; Decker, C.; Keller, L.; Zahouily, K. *Eur. Polym. J.* **2004**, *40*, 493.
29. Decker, C.; Zahouily, K.; Keller, L.; Benfarhi, S.; Bendaikha, T.; Baron, J. *J. Mater. Sci.* **2002**, *37*, 4831.
30. Di Gianni, A.; Bongiovanni, R.; Conzatti, L.; Turri, S. *J. Colloid Inter. Sci.* **2009**, *336*, 455.
31. Benbayer, C.; Saidi-Besbes, S.; Taffin de Givenchy, E.; Amiogani, S.; Guittard, F.; Derdour, A. *J. Colloid Inter. Sci.* **2013**, *408*, 125.
32. Vazquez, A.; López, M.; Kortaberria, G.; Martín, L.; Mondragon, I. *Appl. Clay Sci.* **2008**, *41*, 24.
33. Wang, Y.-Y.; Hsieh, T.-E. *J. Mater. Sci.* **2007**, *42*, 4451.
34. Osman, M. A.; Ploetze, M.; Suter, U. W. *J. Mater. Chem.* **2003**, *13*, 2359.
35. Simons, R.; Qiao, G. G.; Powell, C. E.; Bateman, S. A. *Langmuir* **2010**, *26*, 9023.
36. Bongiovanni, R.; Turcato, E. A.; Di-Gianni, D.; Ronchetti, S. *Prog. Org. Coat.* **2008**, *62*, 336.
37. Lagaly, G. *Solid State Ionics* **1986**, *22*, 43.
38. Akelah, A.; Moet, A. *J. Mater. Sci.* **1996**, *31*, 3589.
39. Zhang, J.; Jiang, D. D.; Wang, D.; Wilkie, C. A. *Polym. Degrad. Stab.* **2006**, *91*, 2665.
40. Zhang, J.; Wilkie, C. A. *Polymer* **2006**, *47*, 5736.
41. Yilmazer, U.; Ozden, G. *Polym. Compos.* **2006**, *27*, 249.
42. Fan, J.; Liu, S.; Chen, G.; Qi, Z. *J. Appl. Polym. Sci.* **2002**, *83*, 66.
43. Samakande, A.; Sanderson, R. D.; Hartmann, P. C. *J. Polym. Sci. A: Polym. Chem.* **2008**, *46*, 7114.
44. Zhong, Y.; Zhu, Z.; Wang, S. Q. *Polymer* **2005**, *46*, 3006.
45. Benbayer, C.; Saïdi-Besbes, S.; Taffin de Givenchy, E.; Amiogani, S.; Guittard, F.; Derdour, A. *Colloid Polym. Sci.* **2014**, *292*, 1711.